

Electronic and structural properties of multiwall carbon nanotubes

Young-Kyun Kwon and David Tománek

*Department of Physics and Astronomy, and Center for Fundamental Materials Research, Michigan State University,
East Lansing, Michigan 48824-1116*

(Received 12 October 1998)

We calculate the potential energy surface, the low-frequency vibrational modes, and the electronic structure of a (5,5)@(10,10) double-wall carbon nanotube. We find that the weak interwall interaction and changing symmetry cause four pseudogaps to open and close periodically near the Fermi level during the soft librational motion at $\nu \approx 30 \text{ cm}^{-1}$. This electron-libration coupling, absent in solids composed of fullerenes and single-wall nanotubes, may yield superconductivity in multiwall nanotubes. [S0163-1829(98)51548-2]

Carbon nanotubes,^{1,2} narrow seamless graphitic cylinders, show an unusual combination of a nanometer-size diameter and millimeter-size length. This topology, combined with absence of defects on a macroscopic scale, gives rise to uncommon electronic properties of individual single-wall nanotubes^{3,4} which, depending on their diameter and chirality, can be either conducting or insulating.⁵⁻⁷ Significant changes in conductivity of these nanowires may be induced by minute geometric distortions⁸ or external fields.⁹ More intriguing effects, ranging from opening of a pseudogap at E_F (Refs. 10 and 11) to orientational melting,¹² have been predicted to occur when identical metallic nanotubes are bundled to a “rope.”¹³ It appears that the many interesting phenomena in single-wall tubes have distracted the attention of theorists from the more abundant multiwall tubes.

Existing investigations of multiwall nanotubes have focused primarily on their growth mechanism,¹⁴⁻¹⁶ as well as changes of the band structure^{17,18} and total energy¹⁹ as the inner tube rotates about or slides along the tube axis. The interwall interaction in a multiwall tube is very similar to the interball interaction in the C_{60} solid, since these structures share the same sp^2 bonding and interwall distance of $\approx 3.4 \text{ \AA}$ found in graphite. While it is well established that C_{60} molecules rotate relatively freely in the solid at room temperature,²⁰ there has been little discussion of the analogous rotation in systems consisting of nanotubes. Only recently, rotations of individual nanotubes in a rope consisting of (10,10) tubes have been discussed.^{11,12} Owing to the uncommon combination of a relatively small energy barrier for rotation and a large mass of macroscopically long nanotubes, individual tubes are unlikely to move as rigid objects in the rope, but rather to bend and twist locally, displacing orientational dislocations that were frozen in during the tube synthesis.

An intriguing effect, namely the formation of a pseudogap at E_F ,^{10,11} has been predicted to occur in ropes of metallic (10,10) nanotubes of D_{10h} symmetry due to the symmetry lowering while forming a triangular lattice. It is interesting to investigate whether the weak intertube interaction, which strongly modifies the low-frequency end of the vibrational spectrum and the density of state near E_F in an infinite three-dimensional lattice of identical nanotubes, may cause even more dramatic effects in a one-dimensional multiwall tube.

Here we show that the interwall coupling, which opens a pseudogap in bundled single-wall nanotubes due to symmetry lowering, may periodically open and close four such pseudo-gaps near E_F in a “metallic” double-wall nanotube during its librations around and vibrations normal to the tube axis. This type of electron-phonon coupling has not been observed in librating molecular crystals of C_{60} fullerenes or (10,10) nanotubes, that are orientationally frustrated. We study the intriguing interplay between geometry and electronic structure during the low-frequency motion of a double-wall nanotube. Our results indicate that the coupling of conduction electrons to soft tube librations and vibrations is caused by periodic symmetry changes, which are unique in this system and may lead to its superconducting behavior.

We focus the following investigation on the (5,5)@(10,10) double-wall nanotube, shown schematically in Fig. 1(a). The individual (5,5) and (10,10) tubes are both metallic and show the preferred “graphitic” interwall separation of 3.4 \AA when nested. Assuming both tubes to be rigid cylinders with parallel axes, the double-wall tube geometry is defined uniquely by the separation of the axes Δr , the axial offset of the inner tube Δz , the orientation of the inner tube φ_{in} and the outer tube φ_{out} with respect to the plane containing the two axes, shown in Fig. 1(a).

To determine the structural and electronic properties of multiwall nanotubes, we used the parametrized tight-binding technique with parameters determined by *ab initio* calculations for simpler structures.²¹ This approach has been found useful to describe minute electronic structure and total energy differences for systems with too large unit cells to handle accurately by *ab initio* techniques. Some of the problems tackled successfully by this technique are the electronic structure and superconducting properties of the doped C_{60} solid²² and the opening of a pseudogap near the Fermi level in a rope consisting of (10,10) nanotubes.¹¹ The band structure energy functional is augmented by pairwise interactions describing both the closed-shell interatomic repulsion and the long-range attractive van der Waals interaction, to correctly reproduce the interlayer distance and the C_{33} modulus of graphite. The adequacy of this approach can be checked independently by realizing that the translation and rotation of individual tubes are closely related to the shear motion of graphite. We expect the energy barriers in tubes to lie close

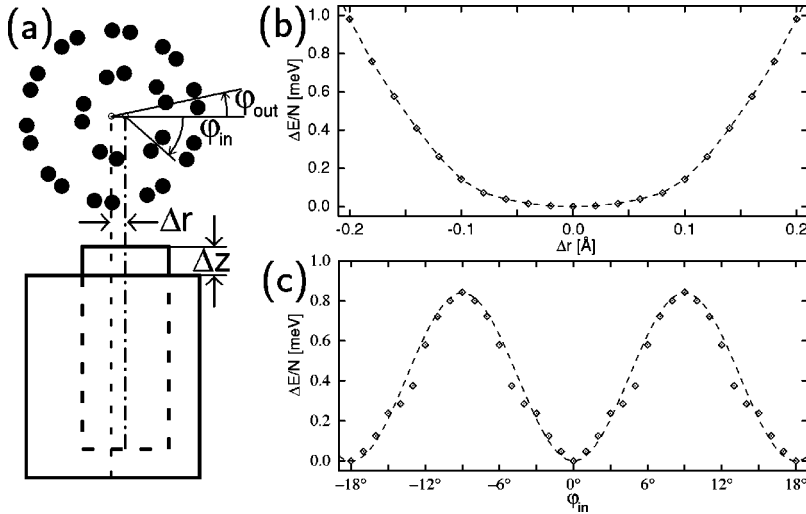


FIG. 1. (a) Schematic view of the (5,5)@(10,10) double-wall tube. The relative radial, axial, and rotational displacement of the inner with respect to the outer tube are described by Δr , Δz , φ_{in} and φ_{out} , respectively. Energy dependence on (b) the separation of the tube axes Δr (for $\Delta z=0$, $\varphi_{in}=0$, $\varphi_{out}=0$), and (c) the orientation of the inner tube φ_{in} (for $\Delta r=0$, $\Delta z=0$, $\varphi_{out}=0$). All energies are given per atom.

to the graphite value which, due to the smaller unit cell, is also easily accessible to *ab initio* calculations.²³

We focus in our calculations on the softest vibrational modes and ignore the deformation of individual tubes from a perfectly cylindrical shape. The dependence of the total energy of the double-wall tube on the distance between the (5,5) and (10,10) tube axes is shown in Fig. 1(b). Even though our results suggest that the system is coaxial in equilibrium, the potential energy is nearly flat for $|\Delta r| \leq 0.1$ Å. For a perfectly straight tube, the shallow potential well would suggest a very soft radial mode to occur with $\nu = 18$ cm⁻¹. At nonzero temperatures, we do not expect the inner tube to be coaxial, but rather to form a helix inside the outer tube. Such a helix would maximize the interwall contact and also could vibrate and rotate locally about its axis. We believe that helical or similar tube distortions of ≤ 0.1 Å are real, but probably are undetectable in transmission electron microscope images.

Due to the low compressibility of tubes along their axis, axial motion of individual nanotubes resembles that of a

rigid body. Even though the activation barrier *per atom* for axial displacement of one tube inside the other is only 0.2 meV,¹⁹ the activation barrier to move the entire rigid nanotube is infinitely high, thus effectively freezing in this particular degree of freedom.

Due to the relatively high symmetry of the coaxial system consisting of a D_{5d} (5,5) nanotube nested inside the D_{10h} (10,10) nanotube, the dependence of the inter-tube interaction on the tube orientation shows a periodicity of 18°. Our results in Fig. 1(c) suggest this interaction to be harmonic, with a relatively low activation barrier for tube rotation of 0.8 meV/atom. Assuming that the outer tube was pinned, the inner tube would exhibit a soft libration with a frequency $\nu_{in} \approx 31$ cm⁻¹. In the opposite case of a fixed inner tube, the heavier outer wall should librate with $\nu_{out} \approx 11$ cm⁻¹. A free double-wall tube should librate with a single frequency $\nu \approx 33$ cm⁻¹.

As in an infinite system consisting of bundled identical nanotubes, we expect also in an individual double-wall nanotube an orientational depinning and melting to occur at suf-

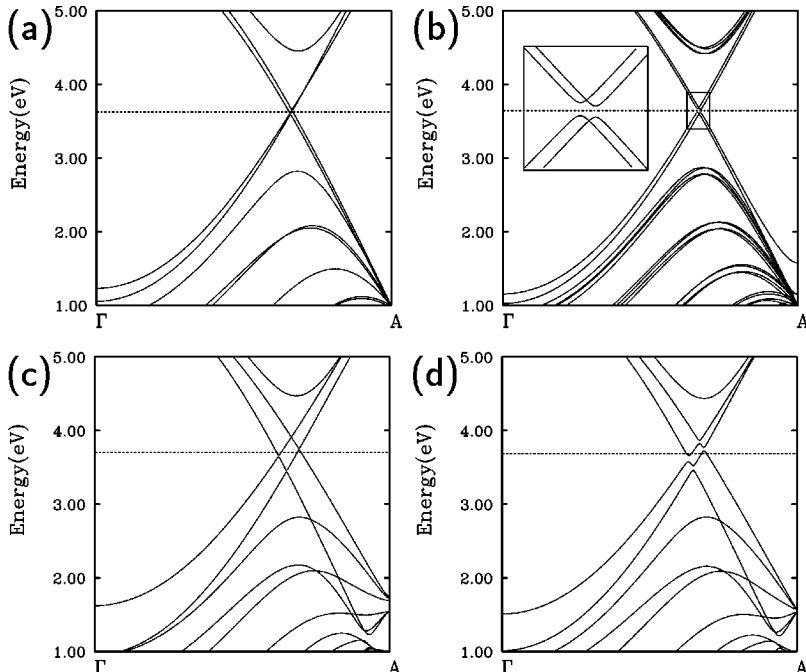


FIG. 2. Band structure of aligned nanotube pairs, along the tube axis. Near degenerate bands with no gap characterize the (5,5)@(10,10) double-wall nanotube without intertube interaction (a). Intertube interaction opens a gap in a pair of (individually metallic) (10,10) nanotubes (b). In presence of intertube interaction, depending on the mutual tube orientation, the (5,5)@(10,10) system may show zero gap in the most symmetric, stable configuration at $\varphi_{in}=0^\circ$ (c), or four pseudogaps in a less symmetric and stable configuration at $\varphi_{in}=3^\circ$ (d). The Fermi level is shown by the dashed line.

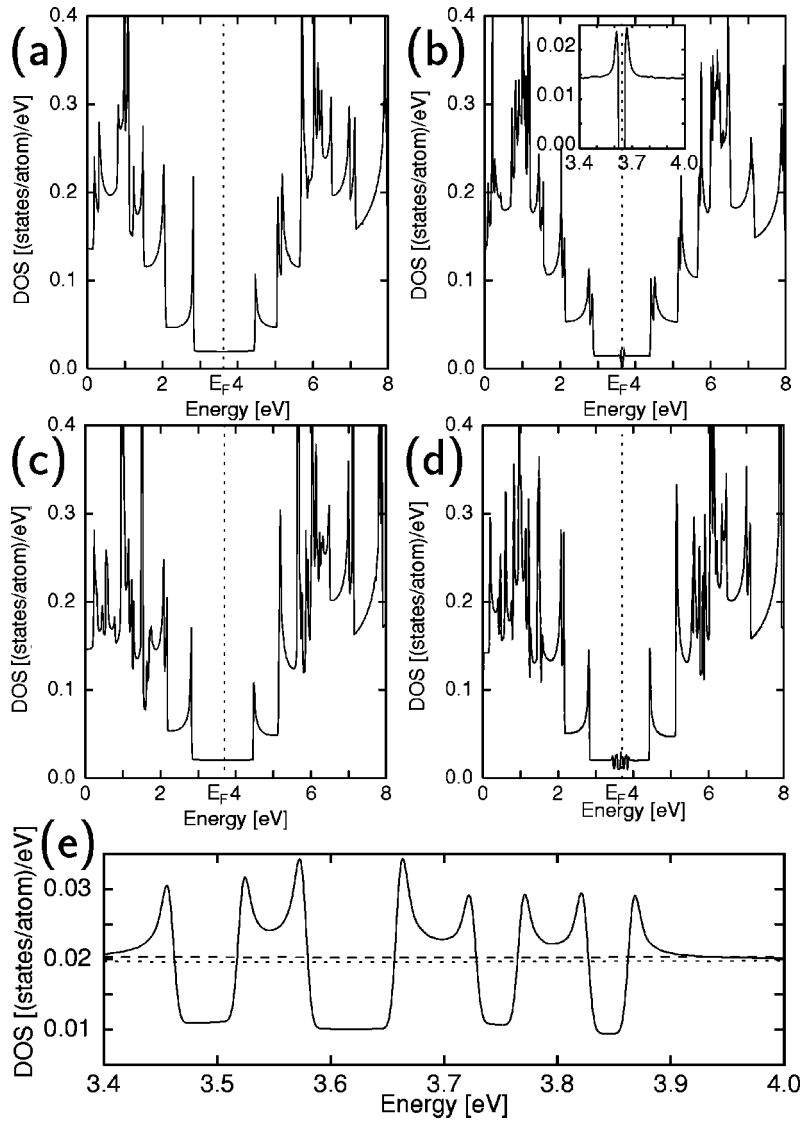


FIG. 3. Density of states of aligned nanotube pairs, corresponding to the band structures in Fig. 2: The (5,5)@(10,10) double-wall tube with no intertube interaction (a); pair of interacting (10,10) nanotubes (b); the (5,5)@(10,10) double-wall tube as a function of mutual tube orientation, for $\varphi_{in}=0^\circ$ (c), and $\varphi_{in}=3^\circ$ (d). The Fermi level is shown by the dashed line. The densities of states of (5,5)@(10,10) tubes near E_F are compared on an expanded energy scale in (e). Appearance of pseudogaps, shown by the solid line for $\varphi_{in}=3^\circ$, is in stark contrast with the flat density of states for $\varphi_{in}=0^\circ$ and $\varphi_{in}=9^\circ$, shown by the long-dashed line. The dotted line indicates the density of states of noninteracting (5,5) and (10,10) tubes.

ficiently high temperatures. The onset of orientational melting at T_{OM} is expected to be qualitatively similar to that described for the infinite lattice of (10,10) nanotubes.^{11,12} Even though the activation barrier for rotation may be small on a *per atom* basis, the relevant quantity in this case is the infinitely high barrier for the entire rigid tube that would lock it in place. In the other extreme of a straight, zero-rigidity tube composed of independent atoms, 0.8 meV/atom activation barrier for rotation would give rise to an orientational melting transition at $T_{OM} \approx 10$ K.

A more realistic estimate of the onset of orientational disorder must consider that multiwall nanotubes, when synthesized, are far from being straight over long distances. As suggested by the potential energy surface for the librational mode in Fig. 1(c), a local twist by $\varphi_{in} > 9^\circ$ results in the nanotube switching locally from one equilibrium orientation to another. Formally, by mapping the orientational coordinate φ_{in} onto the position coordinate x , this process can be described using the Frenkel-Kontorova model used to describe dislocations in strained one-dimensional lattices. Under synthesis conditions at temperatures exceeding 1000 K, we expect substantial finite twists to occur in the individual tubes. Upon forming a multiwall tube, in an attempt to optimize the interwall interaction while minimizing the torsion

energy, orientational dislocations are frozen in at an energy cost of only ≈ 1.0 meV per atom in a ≈ 100 Å long strained region,²⁴ as compared to an optimized straight double-wall tube. Taking a straight, zero-rigidity tube as a reference, we expect T_{OM} to increase from the 10 K value with increasing rigidity. Presence of orientational dislocations, on the other hand, should lower the activation barrier for tube rotations, thus lowering T_{OM} and possibly compensating the effect of nonzero rigidity.

The weak intertube interaction not only induces new vibrational modes, but also modifies significantly the electronic structure near E_F . Individual (5,5) and (10,10) armchair nanotubes, with their respective D_{5d} and D_{10h} symmetries, are metallic. The band structure of each tube is characterized by two crossing linear bands near E_F , one for ‘‘left’’ and one for ‘‘right’’ moving electrons. The band structure of a pair of decoupled (5,5) and (10,10) nanotubes, a mere superposition of the individual band structures, is shown in Fig. 2(a). The linearity of the energy bands in between the van Hove singularities closest to E_F translates into a constant density of states in that energy region, as shown in Fig. 3(a).

It has been argued that the symmetry lowering upon bunching identical metallic (10,10) tubes to a close-packed

lattice causes a pseudogap to open at E_F .^{10,11} As we show in Fig. 2(b), even the weak interaction between two adjacent (10,10) tubes gives rise to a band repulsion. In this lower-symmetry configuration, moreover, a true band gap opens at E_F , as shown in Fig. 3(b).

As we see in Figs. 2(c) and 2(d), switching on the intertube interaction in the (5,5)@(10,10) double-wall tube removes the near degeneracy of the bands near E_F as well. In the most stable orientation, characterized by $\varphi_{in}=0^\circ$, the double-wall system is still characterized by the D_{5d} symmetry of the inner tube. The four bands cross, with a very small change in slope causing the density of states to increase by $\approx 3\%$, as shown in Figs. 3(c) and 3(e). While the same argument also applies to the least stable orientation $\varphi_{in}=9^\circ$, a markedly different behavior is obtained at any other tube orientation that lowers the symmetry. As seen in Fig. 2(d), the symmetry lowering for $\varphi_{in}=3^\circ$ gives rise to four avoided band crossings. This translates into four pseudogaps in the density of states near E_F , as shown in Fig. 3(d) and even better at the expanded energy scale in Fig. 3(e).

We expect that the density of states at the Fermi level should be affected not only by few charged impurities that would shift E_F , but even during the libration motion of the double-wall tube, since the position of the four pseudo-gaps depends significantly on the mutual tube orientation. We also would like to emphasize that the opening and closing of pseudogaps is unique to multi-wall nanotubes and does not occur in single-wall nanotube ropes.^{10,11}

The significance of our results extends well beyond the (5,5)@(10,10) system discussed here. In an n -wall armchair nanotube, we would expect n^2 avoided band crossings to

occur, inducing up to n^2 pseudogaps in the density of states near E_F . These pseudogaps could open and close, depending on the symmetry reduction during tube librations and vibrations.

($n,0$) zig-zag nanotubes are nearly metallic if n is a multiple of three.⁵⁻⁷ If we ignore the curvature-induced gap of few meV at E_F , the bands describing “left” and “right” moving electrons would cross at $\mathbf{k}=\Gamma$. As the intertube interaction is switched on in the “metallic” (9,0)@(18,0) nanotube, the 30 meV gap opens to twice this value at $\varphi_{in}=\varphi_{out}=0^\circ$, and to even a larger value for lower-symmetry configurations. In the semiconducting (8,0)@(17,0) system, on the other hand, the inter-tube interaction reduces the 0.6 eV gap of the noninteracting system by 0.1 eV.

In summary, we calculated the potential energy surface characterizing the interaction between the individual tubes in the (5,5)@(10,10) double-wall nanotube as a function of the interaxis distance and the mutual tube orientation. We found that the weak intertube interaction periodically opens and closes four pseudogaps near E_F due to symmetry lowering during the low-frequency librational motion about and vibrational motion normal to the double-tube axis. The soft librational motion is expected to occur at $\lesssim 30\text{ cm}^{-1}$ below the orientational melting temperature, which marks the onset of relatively free rotations of the individual tubes, probably via axial displacement of orientational dislocations that were frozen in during the tube formation. The strong coupling between the libration mode and the electronic states at the Fermi level, which is apparently absent in nanotube and fullerene crystals, may cause superconductivity in systems containing multiwall nanotubes.

¹Sumio Iijima, Nature (London) **354**, 56 (1991).

²For a general review, see M. S. Dresselhaus, G. Dresselhaus, and P. C. Eklund, *Science of Fullerenes and Carbon Nanotubes* (Academic Press Inc., San Diego, 1996), and references therein.

³S. Iijima and T. Ichihashi, Nature (London) **363**, 603 (1993).

⁴D. S. Bethune, C. H. Kiang, M. S. de Vries, G. Gorman, R. Savoy, J. Vazquez, and R. Beyers, Nature (London) **363**, 605 (1993).

⁵J. W. Mintmire, B. I. Dunlap, and C. T. White, Phys. Rev. Lett. **68**, 631 (1992).

⁶R. Saito, M. Fujita, G. Dresselhaus, and M. S. Dresselhaus, Appl. Phys. Lett. **60**, 2204 (1992).

⁷N. Hamada, S. Sawada, and A. Oshiyama, Phys. Rev. Lett. **68**, 1579 (1992).

⁸C. L. Kane and E. J. Mele, Phys. Rev. Lett. **78**, 1932 (1997).

⁹S. J. Tans, A. R. M. Verschueren, and C. Dekker, Nature (London) **393**, 49 (1998).

¹⁰P. Delaney, H. J. Choi, J. Ihm, S. G. Louie, and M. L. Cohen, Nature (London) **391**, 466 (1998).

¹¹Young-Kyun Kwon, Susumu Saito, and David Tománek, Phys. Rev. B **58**, R13 314 (1998).

¹²Young-Kyun Kwon, David Tománek, Young Hee Lee, Kee Hag Lee, and Susumu Saito, J. Mater. Res. **13**, 2363 (1998).

¹³A. Thess, R. Lee, P. Nikolaev, H. Dai, P. Petit, J. Robert, C. Xu, Y. H. Lee, S. G. Kim, D. T. Colbert, G. Scuseria, D. Tománek, J. E. Fischer, and R. E. Smalley, Science **273**, 483 (1996).

¹⁴Young-Kyun Kwon, Young Hee Lee, Seong Gon Kim, Philippe Jund, David Tománek, and Richard E. Smalley, Phys. Rev. Lett. **79**, 2065 (1997).

¹⁵J.-C. Charlier, A. De Vita, X. Blase, and R. Car, Science **275**, 646 (1997).

¹⁶M. Buongiorno Nardelli, C. Brabec, A. Maiti, C. Roland, and J. Bernholc, Phys. Rev. Lett. **80**, 313 (1998).

¹⁷Riichiro Saito, G. Dresselhaus, and M. S. Dresselhaus, J. Appl. Phys. **73**, 494 (1993).

¹⁸Ph. Lambin, L. Philippe, J. C. Charlier, and J. P. Michenaud, Comput. Mater. Sci. **2**, 350 (1994).

¹⁹J.-C. Charlier and J.-P. Michenaud, Phys. Rev. Lett. **70**, 1858 (1993).

²⁰C. S. Yannoni, R. D. Johnson, G. Meijer, D. S. Bethune, and J. R. Salem, J. Phys. Chem. **95**, 9 (1991); R. Tycko, R. C. Haddon, G. Dabbagh, S. H. Glarum, D. C. Douglass, and A. M. Mujsce, *ibid.* **95**, 518 (1991).

²¹D. Tománek and Michael A. Schluter, Phys. Rev. Lett. **67**, 2331 (1991).

²²M. Schluter, M. Lannoo, M. Needels, G. A. Baraff, and D. Tománek, Phys. Rev. Lett. **68**, 526 (1992).

²³J.-C. Charlier, X. Gonze, and J.-P. Michenaud, Europhys. Lett. **28**, 403 (1994); M. C. Schabel and J. L. Martins, Phys. Rev. B **46**, 7185 (1992).

²⁴Y.-K. Kwon and D. Tománek (unpublished).